Electronic Supplementary Information (ESI)

Bayesian optimization of the composition of the lanthanide metal-organic framework MIL-103 for white-light emission

Yu Kitamura,[a] Hiroki Toshima,[a] Akihiro Inokuchi,[b] and Daisuke Tanaka*[a]

---

a. Department of Chemistry, School of Science, Kwansei Gakuin University, 1 Gakuen-Uegahara, Sanda, Hyogo 669-1330, Japan

b. Program of Computer Science, School of Engineering, Kwansei Gakuin University, 1 Gakuen-Uegahara, Sanda, Hyogo 669-1330, Japan.

Corresponding Author. E-mail: dtanaka@kwansei.ac.jp.

Table of Contents

S1. General information

Chemicals. All reagents were purchased and used without further purification. 1,3,5-Tris(4-carboxyphenyl)benzene (H_3BTB, 98.0%), and *N,N*-dimethylformamide (DMF, 99.95%) were purchased from FUJIFILM Wako Pure Chemical Corporation, Japan. Lanthanide nitrates were purchased from various companies: $Gd(NO_3)_3 \cdot 6H_2O$ (99.95%) and $Tb(NO_3)_3 \cdot 6H_2O$ (99.95%) were purchased from Kanto Chemical Co., Inc., Japan; $Eu(NO_3)_3 \cdot 6H_2O$ (99.9%) was purchased from Kishida Chemical Co., Ltd., Japan.

Characterization. Powder X-ray diffraction (PXRD) patterns were recorded on a Rigaku MiniFlex600 diffractometer at 40 kV and 15 mA using a Cu target tube. The samples were examined without grinding, and the data were collected for 2θ values of 2–30 ° using Cu Kα radiation. The excitation and emission spectra were obtained using a HITACHI F-7000 spectrofluorophotometer. Fluorescence spectrum measurements were chosen on the short wavelength side (295 nm) to avoid an overlap with the fluorescence spectrum due to the small Stokes shift of the ligands. The PXRD patterns were simulated based on single-crystal data using the diffraction crystal module of the Mercury software program (version 3.10), which is available at no charge at http://www.iucr.org.

Bayesian optimization.

Bayesian optimization was performed using GPyOpt with the Gaussian Process framework, GPy, in Ptython. The versions of GPyOpt, GPy, and Python used were 1.2.6, 1.10.0, and 3.8.6, respectively. Given a dataset consisting of samples $\{(\vec{x}_i,\ y_i)\}_{i=1}^{n}$ as input, the Gaussian Process Regression decides the expected value and standard deviation for $f(\vec{x})$ based on, $\left(f(\vec{x}_1),\ f(\vec{x}_2),\dots,f(\vec{x}_n),f(\vec{x})\right)^T \sim \mathcal{N}(0,K)^1$, where K is the n+1-st kernel matrix whose (i,j)-element represents the similarity between $\vec{x}_i$ and $\vec{x}_j$. The Bayesian optimizer in GpyOpt iteratively samples the next $\vec{x}_{n+1}$ which minimizes the acquisition function $\mathbb{E}[min\{f(\vec{x}_1)\} - \tau, 0]$, where τ is the minimum among $f(\vec{x}_1)$, $f(\vec{x}_2),\dots,f(\vec{x}_n)$.

S2. Synthesis

Synthetic conditions 1 (MIL-103(Eu, Gd, Tb)). $Ln(NO_3)_3 \cdot xH_2O$ (Ln = Eu, Gd, or Tb) (17.6 mg, 0.040 mmol) and H_3BTB (5.8 mg, 0.013 mmol) were mixed with 2 mL of DMF/MeOH/H_2O (3:3:0.5) in a 4-mL Teflon-lined stainless-steel container, and the reaction mixture was heated at 80 °C for 48 h. At the end of the heating process, the container was cooled to 30 °C. The heating and cooling times were 5 h and 12 h, respectively. Yield: 55% (MIL103(Eu)), 28% (MIL-103(Gd)), 58% (MIL-103(Tb)) (based on the ligand).

Synthetic conditions 2 (initial screening). $Ln(NO_3)_3 \cdot xH_2O$ (Ln = Eu, Gd, or Tb) (Eu : 9.9×10^{-7}–3.8×10^{-4} mmol, Gd : 0.038–0.040 mmol, Tb : 2.0×10^{-4}–2.5×10^{-3} mmol) and H_3BTB (5.8 mg, 0.013 mmol) were mixed with 2 mL of DMF/MeOH/H_2O (3:3:0.5) in a 4-mL Teflon-lined stainless-steel container, and the reaction mixture was heated at 80 °C for 48 h. At the end of the heating process, the container was cooled to 30 °C. The heating and cooling times were 5 and 12 h, respectively.

Synthetic conditions 3 (optimized synthetic conditions). $Ln(NO_3)_3 \cdot xH_2O$ (Ln = Eu, Gd, or Tb) (Eu : 4.98×10^{-2} mM, 9.95×10^{-7}–1.29×10^{-6} mmol, Gd : 39.93 mM, 0.0375 mmol, Tb : 4.83 mM, 1.74×10^{-4}–2.13×10^{-4} mmol) and H_3BTB (5.8 mg, 0.013 mmol) were mixed with 2 mL of DMF/MeOH/H_2O (3:3:0.5) in a 4-mL Teflon-lined stainless-steel container, and the reaction mixture was heated at 80 °C for 48 h. At the end of the heating process, the container was cooled to 30 °C. The heating and cooling times were 5 and 12 h, respectively.

Synthetic conditions 4 (preparation of a white-light emission at initial screening). $Ln(NO_3)_3 \cdot xH_2O$ (Ln = Eu, Gd, or Tb) (Eu : 1.1×10^{-6} mmol, Gd : 0.040 mmol, Tb : 2.2×10^{-4} mmol) and H_3BTB (5.8 mg, 0.013 mmol) were mixed with 2 mL of DMF/MeOH/H_2O (3:3:0.5) in a 4-mL Teflon-lined stainless-steel container, and the reaction mixture was heated at 80 °C for 48 h. At the end of the heating process, the container was cooled to 30 °C. The heating and cooling times were 5 and 12 h, respectively.

Synthetic conditions 5 (preparation of a white-light emission at Bayesian optimization). $Ln(NO_3)_3 \cdot xH_2O$ (Ln = Eu, Gd, or Tb) (Eu : 1.09×10^{-6} mmol, Gd : 0.0375 mmol, Tb : 1.93×10^{-4} mmol) and H_3BTB (5.8 mg, 0.013 mmol) were mixed with 2 mL of DMF/MeOH/H_2O (3:3:0.5) in a 4-mL Teflon-lined stainless-steel container, and the reaction mixture was heated at 80 °C for 48 h. At the end of the heating process, the container was cooled to 30 °C. The heating and cooling times were 5 and 12 h, respectively.

S3 Initial screening and post-Bayesian optimization screening

Table S1. Initial synthesis screening conditions of the lanthanide metals.

Entry	Eu / mmol	Tb / mmol	Gd / mmol	Entry	Eu / mmol	Tb / mmol	Gd / mmol
1	1.61×10^{-4}	1.86×10^{-3}	0.0378	25	1.11×10^{-5}	5.56×10^{-4}	0.0395
2	1.69×10^{-4}	1.58×10^{-5}	0.0378	26	1.65×10^{-5}	5.51×10^{-4}	0.0395
3	1.77×10^{-4}	1.54×10^{-5}	0.0378	27	2.18×10^{-5}	5.45×10^{-4}	0.0395
4	1.85×10^{-4}	1.49×10^{-5}	0.0378	28	2.70×10^{-5}	5.40×10^{-4}	0.0395
5	1.93×10^{-4}	1.45×10^{-5}	0.0378	29	1.20×10^{-5}	5.98×10^{-4}	0.0394
6	2.01×10^{-4}	1.41×10^{-5}	0.0378	30	1.78×10^{-5}	5.92×10^{-4}	0.0394
7	2.09×10^{-4}	1.37×10^{-5}	0.0378	31	2.35×10^{-5}	5.87×10^{-4}	0.0394
8	2.17×10^{-4}	1.33×10^{-5}	0.0378	32	2.90×10^{-5}	5.81×10^{-4}	0.0394
9	2.41×10^{-4}	1.20×10^{-5}	0.0378	33	1.29×10^{-5}	6.47×10^{-4}	0.0394
10	2.49×10^{-4}	1.16×10^{-5}	0.0378	34	1.92×10^{-5}	6.41×10^{-4}	0.0394
11	2.57×10^{-4}	1.12×10^{-5}	0.0378	35	2.54×10^{-5}	6.35×10^{-4}	0.0394
12	2.65×10^{-4}	1.08×10^{-5}	0.0378	36	3.14×10^{-5}	6.29×10^{-4}	0.0394
13	2.73×10^{-4}	1.04×10^{-5}	0.0378	37	1.41×10^{-5}	7.05×10^{-4}	0.0394
14	2.81×10^{-4}	9.94×10^{-4}	0.0378	38	2.09×10^{-5}	6.98×10^{-4}	0.0394
15	2.89×10^{-4}	9.52×10^{-4}	0.0378	39	2.77×10^{-5}	6.91×10^{-4}	0.0394
16	2.97×10^{-4}	9.10×10^{-4}	0.0378	40	3.42×10^{-5}	6.85×10^{-4}	0.0394
17	3.21×10^{-4}	7.85×10^{-4}	0.0378	41	1.55×10^{-5}	7.74×10^{-4}	0.0393
18	3.29×10^{-4}	7.43×10^{-4}	0.0378	42	2.30×10^{-5}	7.66×10^{-4}	0.0393
19	3.37×10^{-4}	7.02×10^{-4}	0.0378	43	3.04×10^{-5}	7.59×10^{-4}	0.0393
20	3.45×10^{-4}	6.60×10^{-4}	0.0378	44	3.76×10^{-5}	7.52×10^{-4}	0.0393
21	3.53×10^{-4}	6.18×10^{-4}	0.0378	45	1.72×10^{-5}	8.58×10^{-4}	0.0392
22	3.61×10^{-4}	5.77×10^{-4}	0.0378	46	2.55×10^{-5}	8.50×10^{-4}	0.0392
23	3.69×10^{-4}	5.35×10^{-4}	0.0378	47	3.37×10^{-5}	8.42×10^{-4}	0.0392
24	3.77×10^{-4}	4.93×10^{-4}	0.0378	48	4.17×10^{-5}	8.34×10^{-4}	0.0392

Entry	Eu / mmol	Tb / mmol	Gd / mmol	Entry	Eu / mmol	Tb / mmol	Gd / mmol
49	1.11×10^{-5}	5.56×10^{-4}	0.0395	75	1.98×10^{-5}	8.01×10^{-4}	0.0392
50	1.65×10^{-5}	5.51×10^{-4}	0.0395	76	1.98×10^{-5}	8.51×10^{-4}	0.0391
51	2.18×10^{-5}	5.45×10^{-4}	0.0395	77	1.98×10^{-5}	9.01×10^{-4}	0.0391
52	2.70×10^{-5}	5.40×10^{-4}	0.0395	78	1.98×10^{-5}	9.51×10^{-4}	0.0390
53	1.20×10^{-5}	5.98×10^{-4}	0.0394	79	1.98×10^{-5}	1.00×10^{-3}	0.0390
54	1.78×10^{-5}	5.92×10^{-4}	0.0394	80	1.98×10^{-5}	1.05×10^{-3}	0.0389
55	2.35×10^{-5}	5.87×10^{-4}	0.0394	81	1.98×10^{-5}	1.10×10^{-3}	0.0389
56	2.90×10^{-5}	5.81×10^{-4}	0.0394	82	1.98×10^{-5}	1.15×10^{-3}	0.0389
57	1.29×10^{-5}	6.47×10^{-4}	0.0394	83	1.98×10^{-5}	1.20×10^{-3}	0.0388
58	1.92×10^{-5}	6.41×10^{-4}	0.0394	84	1.98×10^{-5}	1.25×10^{-3}	0.0388
59	2.54×10^{-5}	6.35×10^{-4}	0.0394	85	2.77×10^{-5}	5.61×10^{-4}	0.0395
60	3.14×10^{-5}	6.29×10^{-4}	0.0394	86	5.53×10^{-5}	5.56×10^{-4}	0.0395
61	1.41×10^{-5}	7.05×10^{-4}	0.0394	87	8.30×10^{-5}	5.56×10^{-4}	0.0395
62	2.09×10^{-5}	6.98×10^{-4}	0.0394	88	1.11×10^{-5}	5.51×10^{-4}	0.0395
63	2.77×10^{-5}	6.91×10^{-4}	0.0394	89	3.26×10^{-5}	6.51×10^{-4}	0.0396
64	3.42×10^{-5}	6.85×10^{-4}	0.0394	90	6.52×10^{-5}	6.51×10^{-4}	0.0396
65	1.55×10^{-5}	7.74×10^{-4}	0.0393	91	9.68×10^{-5}	6.46×10^{-4}	0.0396
66	2.30×10^{-5}	7.66×10^{-4}	0.0393	92	1.29×10^{-5}	6.46×10^{-4}	0.0396
67	3.04×10^{-5}	7.59×10^{-4}	0.0393	93	4.35×10^{-5}	8.66×10^{-4}	0.0393
68	3.76×10^{-5}	7.52×10^{-4}	0.0393	94	8.59×10^{-5}	8.61×10^{-4}	0.0393
69	1.72×10^{-5}	8.58×10^{-4}	0.0392	95	1.28×10^{-4}	8.56×10^{-4}	0.0393
70	2.55×10^{-5}	8.50×10^{-4}	0.0392	96	1.71×10^{-4}	8.56×10^{-4}	0.0393
71	3.37×10^{-5}	8.42×10^{-4}	0.0392	97	1.97×10^{-6}	7.01×10^{-4}	0.0395
72	4.17×10^{-5}	8.34×10^{-4}	0.0392	98	1.97×10^{-6}	7.51×10^{-4}	0.0394
73	1.98×10^{-5}	7.01×10^{-4}	0.0393	99	1.97×10^{-6}	8.01×10^{-4}	0.0394
74	1.98×10^{-5}	7.51×10^{-4}	0.0392	100	1.97×10^{-6}	8.51×10^{-4}	0.0394

Entry	Eu / mmol	Tb / mmol	Gd / mmol	Entry	Eu / mmol	Tb / mmol	Gd / mmol
101	1.97×10^{-6}	9.01×10^{-4}	0.0393	127	1.67×10^{-6}	2.00×10^{-3}	0.0380
102	1.97×10^{-6}	9.51×10^{-4}	0.0393	128	1.67×10^{-6}	2.10×10^{-3}	0.0379
103	1.97×10^{-6}	1.00×10^{-3}	0.0392	129	1.67×10^{-6}	2.20×10^{-3}	0.0378
104	1.97×10^{-6}	1.05×10^{-3}	0.0392	130	1.67×10^{-6}	2.30×10^{-3}	0.0377
105	1.97×10^{-6}	1.10×10^{-3}	0.0391	131	1.67×10^{-6}	2.40×10^{-3}	0.0376
106	1.97×10^{-6}	1.15×10^{-3}	0.0391	132	1.67×10^{-6}	2.50×10^{-3}	0.0375
107	1.97×10^{-6}	1.20×10^{-3}	0.0390	133	1.67×10^{-6}	3.31×10^{-4}	0.0397
108	1.97×10^{-6}	1.25×10^{-3}	0.0390	134	3.34×10^{-6}	3.26×10^{-4}	0.0397
109	2.76×10^{-6}	5.61×10^{-4}	0.0397	135	4.93×10^{-6}	3.26×10^{-4}	0.0397
110	5.62×10^{-6}	5.61×10^{-4}	0.0397	136	6.60×10^{-6}	3.26×10^{-4}	0.0397
111	8.38.E-06	5.56×10^{-4}	0.0397	137	2.25×10^{-6}	3.97×10^{-4}	0.0396
112	1.10×10^{-5}	5.51×10^{-4}	0.0397	138	4.01×10^{-6}	3.92×10^{-4}	0.0396
113	3.26×10^{-6}	6.51×10^{-4}	0.0396	139	5.93×10^{-6}	3.92×10^{-4}	0.0396
114	6.51×10^{-6}	6.51×10^{-4}	0.0396	140	7.85×10^{-6}	3.92×10^{-4}	0.0396
115	9.67×10^{-6}	6.46×10^{-4}	0.0396	141	2.25×10^{-6}	4.37×10^{-4}	0.0396
116	1.29×10^{-5}	6.46×10^{-4}	0.0396	142	4.43×10^{-6}	4.37×10^{-4}	0.0396
117	4.34×10^{-6}	8.66×10^{-4}	0.0393	143	6.60×10^{-6}	4.37×10^{-4}	0.0396
118	8.58×10^{-6}	8.61×10^{-4}	0.0393	144	8.77×10^{-6}	4.32×10^{-4}	0.0396
119	1.28×10^{-5}	8.56×10^{-4}	0.0393	145	9.90×10^{-7}	2.01×10^{-4}	0.0398
120	1.71×10^{-6}	8.56×10^{-4}	0.0393	146	1.98×10^{-6}	1.96×10^{-4}	0.0398
121	1.67×10^{-6}	1.40×10^{-3}	0.0386	147	2.92×10^{-6}	1.96×10^{-4}	0.0398
122	1.67×10^{-6}	1.50×10^{-3}	0.0385	148	3.91×10^{-6}	1.96×10^{-4}	0.0398
123	1.67×10^{-6}	1.60×10^{-3}	0.0384	149	1.09×10^{-6}	2.21×10^{-4}	0.0400
124	1.67×10^{-6}	1.70×10^{-3}	0.0383	150	2.18×10^{-6}	2.21×10^{-4}	0.0398
125	1.67×10^{-6}	1.80×10^{-3}	0.0382	151	3.27×10^{-6}	2.21×10^{-4}	0.0398
126	1.67×10^{-6}	1.90×10^{-3}	0.0381	152	4.36×10^{-6}	2.21×10^{-4}	0.0398

Entry	Eu / mmol	Tb / mmol	Gd / mmol	Entry	Eu / mmol	Tb / mmol	Gd / mmol
153	2.18×10^{-6}	4.37×10^{-4}	0.0396	155	6.49×10^{-6}	4.37×10^{-4}	0.0396
154	4.36×10^{-6}	4.37×10^{-4}	0.0396	156	8.61×10^{-6}	4.32×10^{-4}	0.0396

Table S2. Synthesis conditions for the lanthanide metals based on Bayesian optimization.

Entry	Eu /μL	Tb /μL	Gd /μL	Eu / mmol	Tb / mmol	Gd / mmol
1	20	36	940	9.95×10^{-7}	1.74×10^{-4}	0.0375
2	20	37	940	9.95×10^{-7}	1.84×10^{-4}	0.0375
3	20	40	940	9.95×10^{-7}	1.93×10^{-4}	0.0375
4	20	44	940	9.95×10^{-7}	2.13×10^{-4}	0.0375
5	22	40	940	1.09×10^{-6}	1.93×10^{-4}	0.0375
6	22	44	940	1.09×10^{-6}	2.13×10^{-4}	0.0375
7	24	36	940	1.19×10^{-6}	1.74×10^{-4}	0.0375
8	24	38	940	1.19×10^{-6}	1.84×10^{-4}	0.0375
9	24	44	940	1.19×10^{-6}	2.13×10^{-4}	0.0375
10	26	37	940	1.29×10^{-6}	1.74×10^{-4}	0.0375

S4 Synthesis of a single MIL-103(Eu, Gd, or Tb)

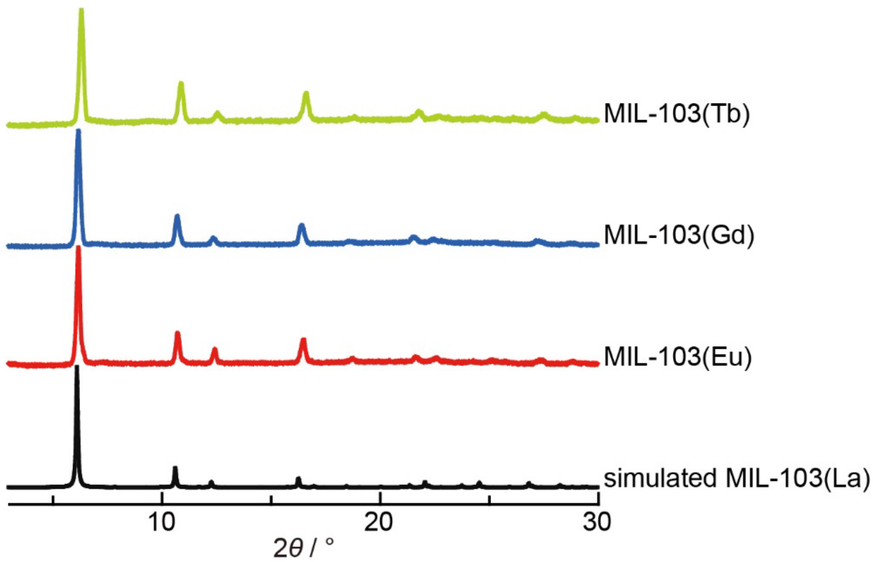

Fig. S1. PXRD patterns of MIL-103(Eu, Gd, or Tb). Patterns for La(BTB)(H_2O) were simulated from reported crystal structures.

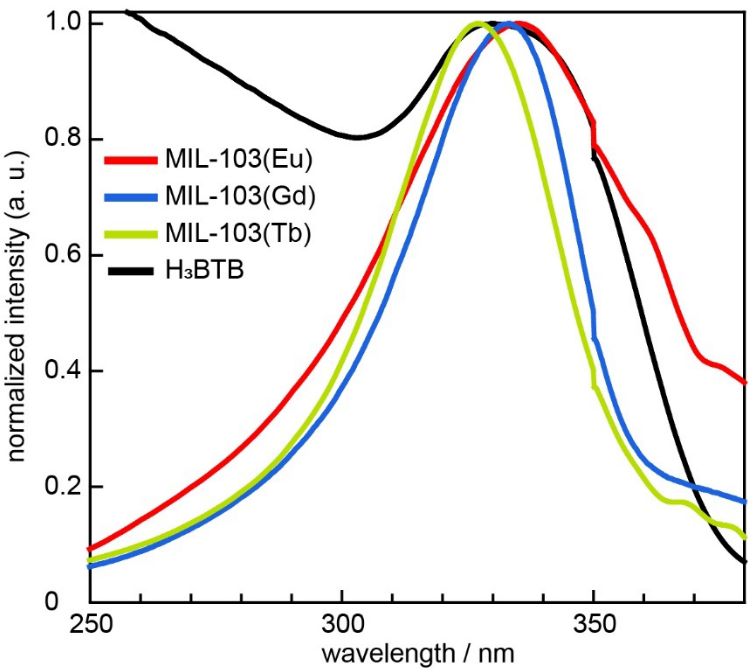

Fig. S2. Excitation spectra of MIL-103(Eu,Gd, Tb) and H_3BTB. Fluorescence wavelength of MIL-103(Eu), MIL-103(Gd), MIL-103(Tb) and H_3BTB were 615, 615, 545, and 395 nm, respectively.

S5 Initial screening synthesis of MIL-103 exhibiting white-light emission

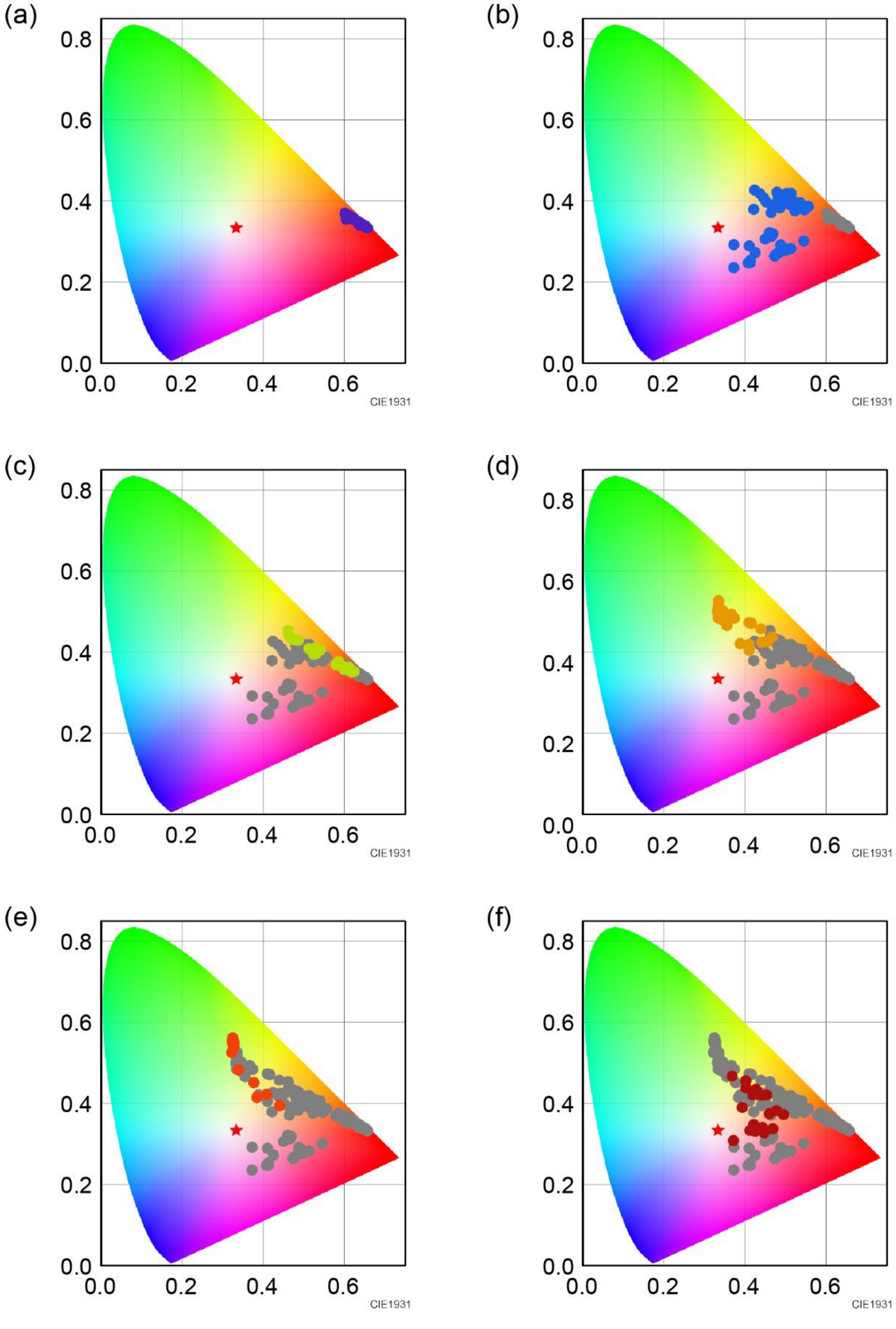

Fig. S3. CIE chromaticity diagram for trial experiments 1–6. (a) 1st trial. (b) 2nd trial. (c) 3rd trial. (d) 4th trial. (e) 5th trial. (f) 6th trial.

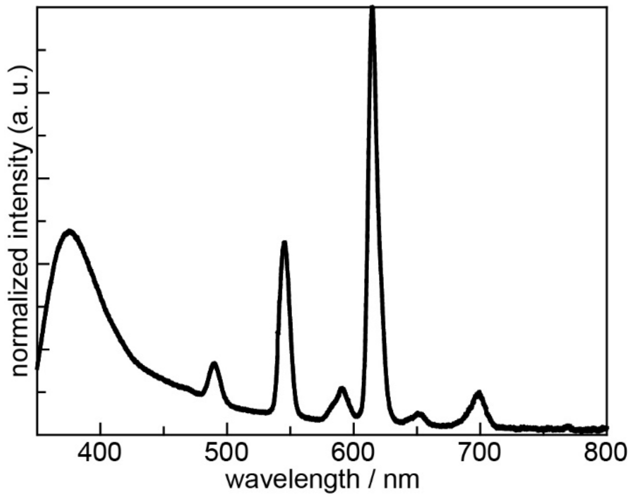

Fig. S4. Emission spectra of MIL-103($Eu_xGd_yTb_z$; Eu = 2.7×10^{-5}, Tb = 5.6×10^{-3}, Gd = 9.94×10^{-1}) (entry 149 in Table S1) which was the closest to white-light emission in the initial screening. Excitation wavelength was 295 nm.

S6 Bayesian optimization of composition of MIL-103 showing white-light emission

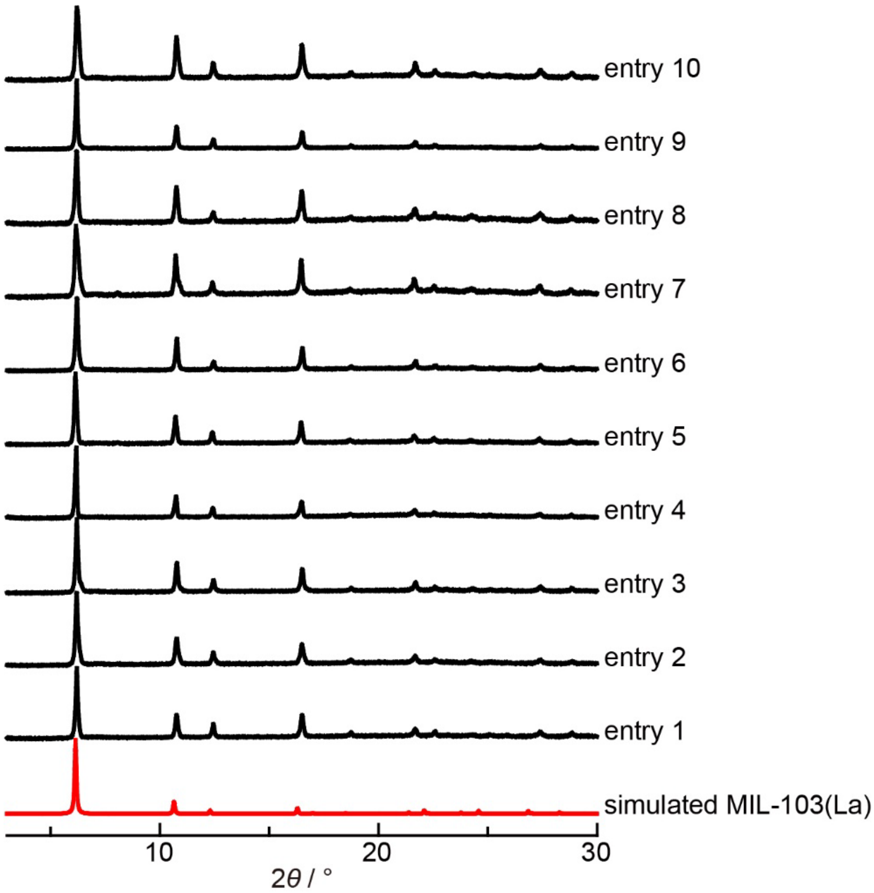

Fig. S5. PXRD pattern of MIL-103 synthesized based on optimal conditions using Bayesian optimization. For detailed conditions of each entry, see Table S2. Patterns for La(BTB)(H_2O) were simulated from reported crystal structures.

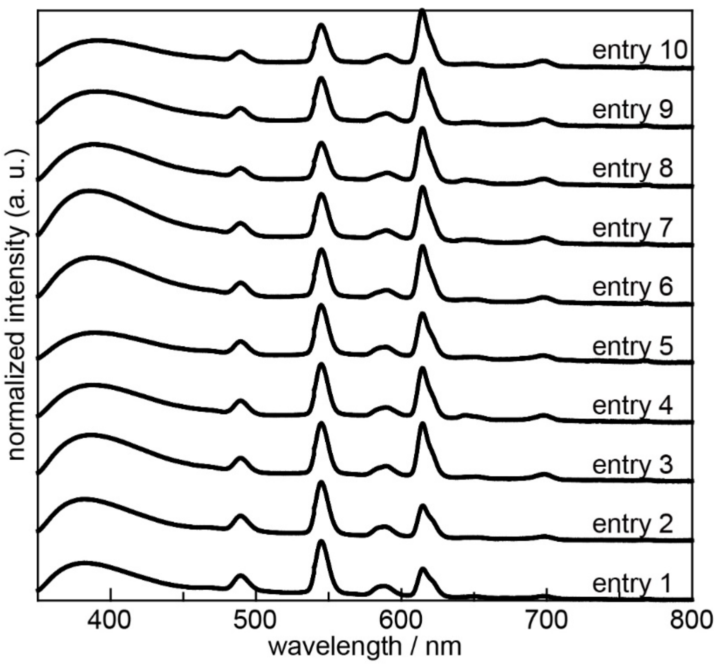

Fig. S6. Emission spectra of MIL-103 synthesized based on optimal conditions by Bayesian optimization. For detailed conditions of each entry, see Table S2.